[DOI]10.12016/j.issn.2096-1456.202550454

·基础研究·

新北美圣草苷对牙周炎小鼠牙槽骨吸收和肠道菌群的影响

伍玉，　袁志瑶，　张杨珩，　闫福华
南京大学医学院附属口腔医院，南京市口腔医院牙周病科，南京大学口腔医学研究所，江苏 南京（210008）

【摘要】　目的　探讨新北美圣草苷（neoeriocitrin，Neo）对小鼠实验性牙周炎的作用及安全性，为牙周炎治疗新型候选药物提供实验依据。**方法**　本研究已获得实验动物福利与伦理安全委员会批准。建立C57BL/6J小鼠牙周炎模型，并设置对照组、牙周炎模型组和3个Neo治疗组（5、10、20 mg/kg Neo）。干预14 d后，通过微型电子计算机断层扫描（micro-computed tomography，micro-CT）分析牙槽骨吸收情况；苏木精-伊红（hematoxylin-eosin，HE）、Masson染色观察牙周组织病理变化；抗酒石酸酸性磷酸酶（tartrate-resistant acid phosphatase staining，TRAP）染色观察破骨细胞；酶联免疫吸附测定（enzyme-linked immunosorbent assay，ELISA）检测血清炎症因子[肿瘤坏死因子-α（tumor necrosis factor-α，TNF-α）、白细胞介素-6（interleukin-6，IL-6）、白细胞介素-1β（interleukin-1β，IL-1β）、白细胞介素-10（interleukin-10，IL-10）]水平；16S rRNA测序分析肠道菌群变化；并通过多器官的HE染色以及结肠紧密连接蛋白（zonula occludens-1，ZO-1）的免疫组化染色评估其生物安全性。**结果**　与牙周炎模型组相比，10 mg/kg Neo治疗组的牙槽骨吸收显著减轻，表现为釉牙骨质界（cemento enamel junction，CEJ）至牙槽嵴顶（alveolar bone crest，ABC）的距离（CEJ-ABC）缩短，骨密度（bone mineral density，BMD）、骨体积分数（bone volume fraction，BV/TV）和骨小梁厚度（trabecular thickness，Tb.Th）增加；牙周组织炎症细胞浸润减少、胶原纤维排列改善、破骨细胞数量显著减少；血清促炎因子TNF-α和IL-6水平降低。此外，10 mg/kg Neo干预可调节肠道菌群结构，且未引起明显的多器官毒性或肠道屏障功能损伤。**结论**　Neo可通过抑制牙槽骨吸收、减轻牙周组织炎症、调节系统免疫和改善肠道菌群，有效缓解小鼠牙周炎的进展，且具有良好的生物安全性，是一种具有潜力的牙周炎治疗候选药物。

【关键词】　新北美圣草苷；　牙周炎；　骨吸收；　炎症因子；　肠道菌群；　口-肠轴；　天然化合物；　破骨细胞
【中图分类号】　R78　**【文献标志码】**　A　**【文章编号】**　2096-1456（2026）03-0226-11
【引用著录格式】　伍玉，袁志瑶，张杨珩，等. 新北美圣草苷对牙周炎小鼠牙槽骨吸收和肠道菌群的影响[J]. 口腔疾病防治, 2026, 34(3): 226-236. doi:10.12016/j.issn.2096-1456.202550454.

微信公众号

Effects of neoeriocitrin on alveolar bone loss and gut microbiota in mice with periodontitis

WU Yu, YUAN Zhiyao, ZHANG Yangheng, YAN Fuhua.　Department of Periodontology, Nanjing Stomatological Hospital, Affiliated Hospital of Medical School, Institute of Stomatology, Nanjing University, Nanjing 210008, China
Corresponding author: YAN Fuhua, Email: yanfh@nju.edu.cn

【Abstract】　Objective　To investigate the inhibitory effect of neoeriocitrin (Neo) on ligature-induced experimental periodontitis in mice and evaluate its biosafety, providing experimental evidence for novel candidate drugs in periodontitis treatment. **Methods**　This study has been approved by the Animal Welfare and Ethical Safety Committee. A periodontitis model was established in C57BL/6J mice using silk ligation. The mice were divided into control, periodontitis model, and three Neo treatment groups (5, 10, 20 mg/kg Neo). After 2 weeks of intervention, alveolar bone resorption was analyzed by micro-computed tomography (micro-CT); periodontal tissue pathological changes were observed *via*

【收稿日期】2025-09-30；　**【修回日期】**2025-11-11
【基金项目】国家自然科学基金项目（82270979）；江苏省医学重点学科建设单位基金项目（JSDW202246）
【作者简介】伍玉，博士研究生在读，Email：Cristina_wuyu@hotmail.com
【通信作者】闫福华，教授，博士，Email：yanfh@nju.edu.cn

hematoxylin-eosin (HE) and Masson staining; osteoclasts were counted using tartrate-resistant acid phosphatase staining; serum inflammatory factor levels [tumor necrosis factor-α (TNF-α), interleukin-6 (IL-6), interleukin-1β (IL-1β), interleukin-10 (IL-10)] were detected by enzyme-linked immunosorbent assay; gut microbiota changes were analyzed by 16S rRNA sequencing; and biosafety was assessed through HE staining of the heart, liver, spleen, lung, kidney, and colon, as well as zonula occludens-1 (ZO-1) immunohistochemical staining of the colon. **Results** Compared with the periodontitis model group, the 10 mg/kg Neo treatment group showed significantly alleviated alveolar bone resorption, manifested as reduced cementoenamel junction to alveolar bone crest distance, increased bone mineral density, bone volume fraction, and trabecular thickness. Additionally, reduced inflammatory cell infiltration, improved collagen fiber arrangement, and a significantly decreased number of osteoclasts were observed in periodontal tissues. Serum levels of pro-inflammatory factors TNF-α and IL-6 were also reduced. Furthermore, 10 mg/kg Neo intervention modulated the gut microbiota structure without causing significant multi-organ toxicity or impairing intestinal barrier function. **Conclusion** Neo can effectively mitigate the progression of experimental periodontitis by inhibiting alveolar bone resorption, reducing periodontal tissue inflammation, modulating systemic immunity, and improving gut microbiota. With good biosafety, Neo is a promising candidate drug for the treatment of periodontitis.

【Key words】 neoeriocitrin; periodontitis; bone resorption; inflammatory factors; gut microbiota; oral-gut axis; natural compound; osteoclast

J Prev Treat Stomatol Dis, 2026, 34(3): 226-236.

【Competing interests】 The authors declare no competing interests.

This study was supported by the grants from National Natural Science Foundation of China (No. 82270979) and Jiangsu Provincial Medical Key Discipline Cultivation Unit (No. JSDW202246).

牙周炎是一种以牙周支持组织破坏为特征的慢性炎症性疾病[1]，其主要发病机制源于龈下菌斑微生物与宿主免疫应答之间的失衡，最终导致牙槽骨吸收和牙丧失，是成年人失牙的首要原因[2-3]。近年研究表明，牙周炎与多种全身系统性疾病存在双向关联，这一过程可能由口腔病原微生物的异位定植和随之引发的系统性炎症反应所介导[4]。尤其值得注意的是，唾液微生物群可向肠道转移，所形成的“口-肠轴”在牙周炎相关的骨质疏松和结肠炎等疾病中起重要作用[5-6]。

目前牙周炎的基础治疗主要依赖龈下刮治和根面平整以机械清除生物膜，但该疗法对部分易感患者效果有限。抗生素等现有药物的耐药性问题限制了其临床应用[7-8]。因此，开发包括局部或全身给药在内的辅助治疗策略显得尤为重要[9-10]。天然化合物如恩贝酸[11]、山奈酚[12]、大麻二酚[13]和淫羊藿苷[14]，因其抗炎、免疫调节和骨吸收抑制活性，同时兼具来源广泛和不良反应较少的特点，逐渐成为牙周炎防治的研究热点。

新北美圣草苷（neoeriocitrin，Neo）是一种从骨碎补或柑橘类水果中提取的黄酮类化合物[15-16]。已有研究证实，该化合物不仅具有抗炎和抗氧化特性[17-18]，还能显著促进小鼠胚胎成骨细胞前体细胞的增殖和碱性磷酸酶活性，上调成骨相关基因Ⅰ型胶原（type Ⅰ collagen，Coll Ⅰ）、Runt相关转录因子2（Runt-related transcription factor 2，Runx2）和骨钙素（osteocalcin，OCN）的表达，并部分逆转PD98059诱导的成骨分化抑制[19]。此外，Neo可抑制骨细胞样细胞系中核因子κ-B配体受体致活剂（receptor activator of nuclear factor kappa-B ligand，RANKL）与骨硬化蛋白（sclerostin，SOST）的mRNA表达[20]。本课题组前期研究结果表明，Neo能有效促进人牙髓干细胞的成骨分化，加速颅骨再生过程，且未观察到明显不良反应[21]。本研究通过构建小鼠实验性牙周炎模型，从牙槽骨吸收、牙周组织病理改变、破骨细胞活化、系统性炎症水平、肠道菌群结构以及多器官安全性等多个维度，综合评价Neo对牙周炎的影响，旨在为其作为牙周炎治疗新型候选药物提供实验依据。

1　材料和方法

1.1　实验动物及主要试剂、仪器

本研究经南京农业大学实验动物福利与伦理委员会批准（审批号：PZW2025016），所有动物实验均在南京农业大学实验动物中心无特定病原体（specific pathogen free，SPF）级屏障环境动物房中开展。选用20只6周龄雄性C57BL/6J小鼠，购自北京维通利华实验动物技术有限公司（合格证号：

20250611AbZZ06000000073）。Neo（PS1276，普思生物，中国）；4%多聚甲醛（BL539A，Biosharp，中国）；乙二胺四乙酸（ethylenediamine tetraacetic acid，EDTA）脱钙液（BL616B，Biosharp，中国）；苏木精-伊红（hematoxylin-eosin，HE）染液套装（S191003，皮诺飞生物，中国）；Masson染色液套装（S191006，皮诺飞生物，中国）；抗酒石酸酸性磷酸酶（tartrate-resistant acid phosphatase，TRAP）染色试剂盒（S191050，皮诺飞生物，中国）；紧密连接蛋白（zonula occludens-1，ZO-1）抗体（一抗兔抗鼠，21773-1-AP，Proteintech，中国）；白细胞介素（interleukin，IL）-1β、IL6、IL10和肿瘤坏死因子α（tumor necrosis factor-α，TNF-α）的酶联免疫吸附测定（enzyme-linked immunosorbent assay，ELISA）试剂盒（JL18442，JL20268，JL20242，JL10484，江莱生物，中国）；MagBeads FastDNA Kit for Soil试剂盒（116564384，MP Biomedicals，美国）；微型电子计算机断层扫描（micro-computed tomography，micro-CT）扫描仪（SkyScan 1176，Bruker，德国）；脱水机（JT-12S，武汉俊杰电子有限公司，中国）；包埋机（JB-L5，武汉俊杰电子有限公司，中国）；病理切片机（RM2016，Leica，德国）；Nanodrop超微量紫外可见分光光度计（NC2000，Thermo Scientific，美国）。

1.2　实验方法

1.2.1　实验性牙周炎的构建和分组　20只6周龄雄性C57BL/6J小鼠经7 d适应性饲养后，随机分为5组（每组4只小鼠）：① 对照组（Ctrl组）：无丝线结扎+生理盐水灌胃；②牙周炎模型组（Lig组）：丝线结扎+生理盐水灌胃；③ Lig+Neo-5组：丝线结扎+5 mg/kg Neo灌胃；④ Lig+Neo-10组：丝线结扎+10 mg/kg Neo灌胃；⑤ Lig+Neo-20组：丝线结扎+20 mg/kg Neo灌胃。Neo的给药剂量参考了化学结构相似的黄酮类化合物在小鼠骨骼与关节炎症模型中的有效剂量范围[22-23]。所有小鼠在异氟烷麻醉下，使用5-0丝线结扎双侧上颌第二磨牙，对照组结扎后立即拆除丝线。各组每日灌胃100 μL相应溶液，连续干预14 d。其间每日检查结扎丝线状态，脱落者立即重新结扎。

1.2.2　样本采集与处理　给药14 d后，以异氟烷麻醉小鼠并摘除眼球采集全血（0.7~1.0 mL/只），静置1 h后，4 ℃，3 500 rpm离心15 min，收集血清并于-80 ℃保存，用于后续炎症因子检测。取双侧上颌骨，4%多聚甲醛固定，用于micro-CT扫描和组织学分析；同时采集心、肝、脾、肺、肾和结肠组织，同法固定并保存，用于组织学检查；盲肠内容物收集于无菌EP管，-80 ℃冻存，用于菌群分析。

1.2.3　上颌骨micro-CT扫描与骨参数分析　双侧上颌骨经4%多聚甲醛固定48 h后，使用Bruker SkyScan 1176系统进行扫描，扫描参数：电压50 kV、电流455 μA、分辨率18 μm。通过DataViewer软件和CT-An软件进行三维重建和影像分析，选取上颌第二磨牙近中根尖1/3区域的牙槽骨作为感兴趣区域（region of interest，ROI），并测量以下参数：釉牙骨质界（cemento enamel junction，CEJ）至牙槽嵴顶（alveolar bone crest，ABC）的距离（CEJ-ABC），用以评估附着丧失；同时分析骨密度（bonemineral density，BMD）、骨体积分数（bone volume fraction，BV/TV）和骨小梁厚度（trabecular thickness，Tb.Th），以综合评价牙槽骨吸收情况。

1.2.4　上颌骨组织学分析　Micro-CT扫描后的上颌骨样本置于10% EDTA溶液中脱钙，每2~3 d更换脱钙液，至针刺无阻力。随后进行脱水、透明、石蜡包埋，并制备4 μm厚切片。按试剂盒说明依次进行HE染色、Masson染色和TRAP染色。

1.2.5　血清炎症因子检测　采用ELISA试剂盒，按说明书检测血清中TNF-α、IL-6、IL-1β和IL-10的浓度。

1.2.6　肠道菌群16S rRNA测序　委托上海派森诺生物科技有限公司完成。使用MagBeads FastDNA Kit for Soil试剂盒提取盲肠内容物基因组DNA，0.8%琼脂糖凝胶电泳进行分子大小判断，利用Nanodrop对DNA进行定量。以338F和806R引物扩增16S rRNA V3-V4区，建库使用Illumina公司的TruSeq Nano DNA LT Library Prep Kit，质检合格后于Illumina NovaSeq平台进行2×250 bp双端测序。原始数据经R软件和QIIME2软件进行数据分析，包括去引物、质控、去噪、拼接和去嵌合体，生成扩增子序列变体（amplicon sequence variants，ASVs）特征表以及丰度数据表格。α多样性组间差异采用Wilcoxon检验；通过Bray-Curtis距离法进行主成分分析（principal coordinates analysis，PCoA）；使用线性判别分析效应大小（linear discriminant analysis effect size，LEfSe）识别组间差异菌属。

1.2.7　多器官组织学与结肠屏障功能检测　心、肝、脾、肺、肾和结肠组织经4%多聚甲醛固定后，常规石蜡包埋、切片，进行HE染色。结肠切片额外进行ZO-1免疫组化染色，Image J软件对ZO-1表达进行半定量分析，以评估肠道屏障完整性。

1.3　统计学分析

所有数据以均值±标准差（$\bar{x}\pm s$）表示，使用GraphPad Prism 9.5软件处理。使用Shapiro-Wilk检验评估正态性，使用Levene检验评估方差的齐性。若数据满足正态分布且方差齐，则采用单因素方差分析进行多组间比较，并使用Tukey检验进行两两比较；若数据不满足正态分布和/或方差不齐，则采用非参数的Kruskal-Wallis检验，并使用Dunn's检验进行两两比较。检验水准$\alpha = 0.05$。

2　结　果

2.1　Neo对牙周炎小鼠牙槽骨吸收的影响

为评估Neo对丝线结扎诱导的牙周炎小鼠牙槽骨吸收的影响，本研究采用micro-CT分析了小鼠上颌第二磨牙区域的骨组织。结果显示，与对照组相比，牙周炎模型组小鼠CEJ至ABC的距离显著增大（$P<0.05$），而BMD、BV/TV和Tb.Th均明显降低（$P<0.05$），表明小鼠实验性牙周炎模型构建成功。Neo干预后，5 mg/kg与10 mg/kg剂量组均能明显改善所有观测的骨参数，其中10 mg/kg剂量组的改善效果最为显著，而20 mg/kg剂量组仅提升了BMD与BV/TV（图1）。结果表明，每日灌胃10 mg/kg Neo可最有效地减轻牙周炎引发的牙槽骨吸收。

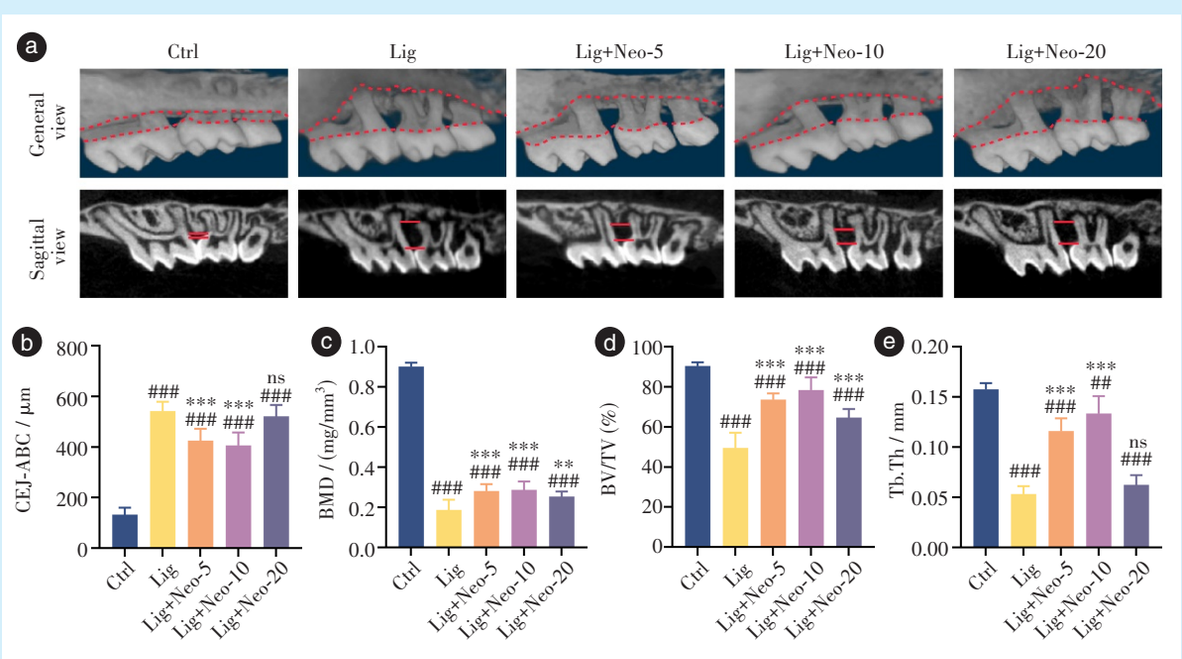

a: representative micro-computed tomography three-dimensional reconstruction and two-dimensional sagittal section images of the maxillae in mice from each group. Dotted line: distance from the buccal alveolar bone crest to the cemento enamel junction; solid line: distance from the alveolar bone crest to the cemento enamel junction. b: distance from the CEJ to the ABC of the maxillary second molar. c – e: quantitative statistical analysis of BMD, BV/TV, and Tb.Th in the alveolar bone at the apical 1/3 region of the mesial root of the maxillary second molar. Ctrl group: mice received saline gavage without silk ligation; Lig group: mice with silk ligation received saline gavage; Lig + Neo-5 group: mice with silk ligation received 5 mg/kg Neo gavage; Lig + Neo-10 group: mice with silk ligation received 10 mg/kg Neo gavage; Lig + Neo-20 group: mice with silk ligation received 20 mg/kg Neo gavage. Neo: neoeriocitrin; CEJ-ABC: cemento enamel junction to alveolar bone crest distance; BMD: bone mineral density; BV/TV: bone volume fraction; Tb.Th: trabecular thickness. Compared with the Ctrl group, ##: $P < 0.01$, ###: $P < 0.001$. Compared with the Lig group, **: $P < 0.01$, ***: $P < 0.001$, ns: $P > 0.05$

Figure 1　Effect of neoeriocitrin on alveolar bone resorption in mice with periodontitis

图1　新北美圣草苷对牙周炎小鼠牙槽骨吸收的影响

2.2　Neo对牙周炎小鼠牙周组织病理变化的影响

为评估牙周组织病理学改变，本研究对小鼠上颌骨样本进行了HE和Masson染色分析。结果显示，对照组牙周组织结构正常，无明显炎症。牙周炎模型组则出现典型的牙周炎病理特征，包括大量炎症细胞浸润、上皮钉突增生、附着丧失和胶

原纤维排列紊乱。经Neo干预后，各剂量组均能减轻牙周组织破坏，其中5 mg/kg与10 mg/kg组效果明显，且后者改善最为显著；20 mg/kg组亦有一定缓解作用，但效果相对较弱（图2）。以上结果表明，Neo能够有效减轻牙周炎引起的软组织结构破坏，且10 mg/kg剂量表现出最优的保护效应。

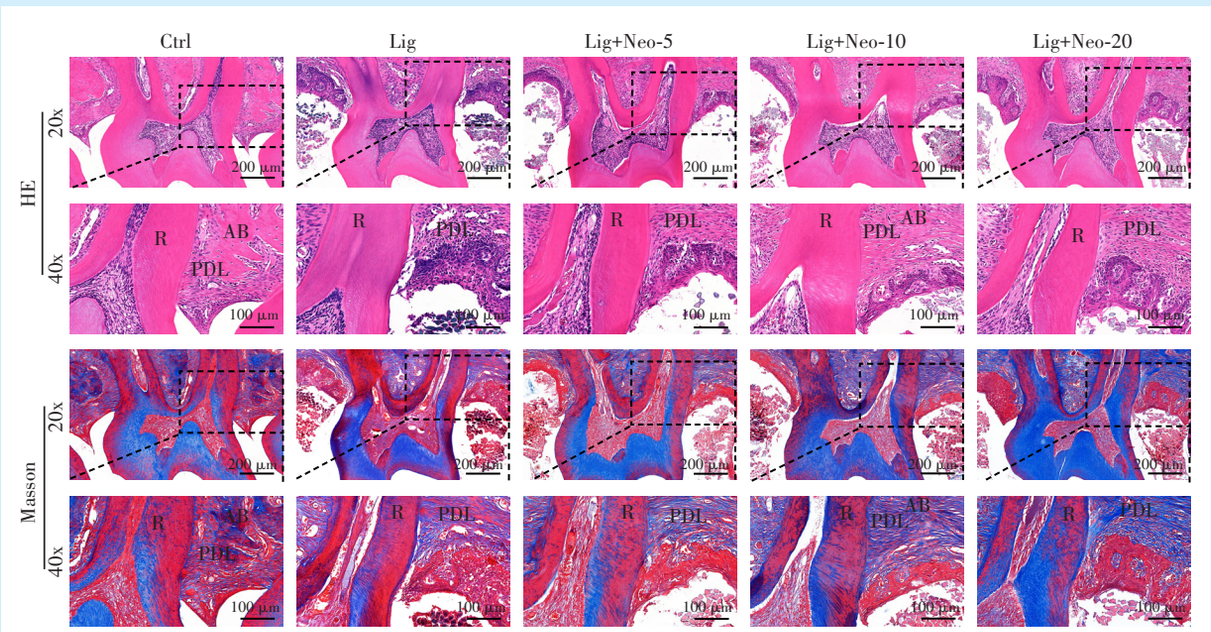

HE and Masson staining images of the maxillary second molars in mice from each group. Scale bars: upper panel = 200 μm, lower panel = 100 μm. Ctrl group: mice received saline gavage without silk ligation; Lig group: mice with silk ligation received saline gavage; Lig + Neo-5 group: mice with silk ligation received 5 mg/kg Neo gavage; Lig + Neo-10 group: mice with silk ligation received 10 mg/kg Neo gavage; Lig + Neo-20 group: mice with silk ligation received 20 mg/kg Neo gavage. Neo: neoeriocitrin; HE: hematoxylin-eosin; AB: alveolar bone; PDL: periodontal ligament; R: root

Figure 2　Effect of neoeriocitrin on pathological changes in periodontal tissues of mice with periodontitis

图2　新北美圣草苷对牙周炎小鼠牙周组织病理变化的影响

2.3　Neo对牙周炎小鼠牙周组织中破骨细胞的影响

为探究Neo对牙周组织中破骨细胞的影响，本研究对小鼠牙周组织进行了TRAP染色。结果显示，与对照组相比，牙周炎模型组牙槽骨表面破骨细胞数量显著增多。经Neo干预后，5、10及20 mg/kg各剂量组在根分叉区和远中邻面牙槽骨的破骨细胞数量均较牙周炎模型组减少，其中以10 mg/kg剂量组的抑制效果最为显著（图3）。该结果提示Neo能够有效抑制破骨细胞活性，与前述牙槽骨吸收减轻的结果相一致。

2.4　Neo对牙周炎小鼠血清炎症因子水平的影响

为分析Neo对系统性炎症的影响，本研究通过ELISA检测了小鼠血清中TNF-α、IL-6、IL-1β和IL-10的含量。结果显示，与对照组比较，牙周炎模型组TNF-α和IL-6水平显著升高（$P<0.05$），IL-1β与IL-10则无显著变化。Neo干预后，在TNF-α水平上，5 mg/kg与10 mg/kg剂量组均能使其显著降低（$P<0.05$）；在IL-6水平上，仅10 mg/kg干预能显著降低其水平（$P<0.05$）；各剂量Neo对IL-1β与IL-10均无显著影响（图4）。

2.5　Neo对牙周炎小鼠肠道菌群的影响

为探究Neo对牙周炎小鼠肠道菌群的影响，本研究对小鼠盲肠内容物进行了16S rRNA测序分析。Alpha多样性分析显示，与对照组相比，牙周炎模型组的Chao1、Shannon、Observed_species等指数均显著降低，表明牙周炎导致小鼠肠道菌群丰富度和均匀度下降。而与牙周炎模型组相比，不同剂量Neo给药组的上述指数均出现回升（图5a），提示菌群结构得到改善。Beta多样性的PCoA分析显示牙周炎模型组与对照组和各给药组明显分离，表明牙周炎改变了菌群结构，而Neo干预能有

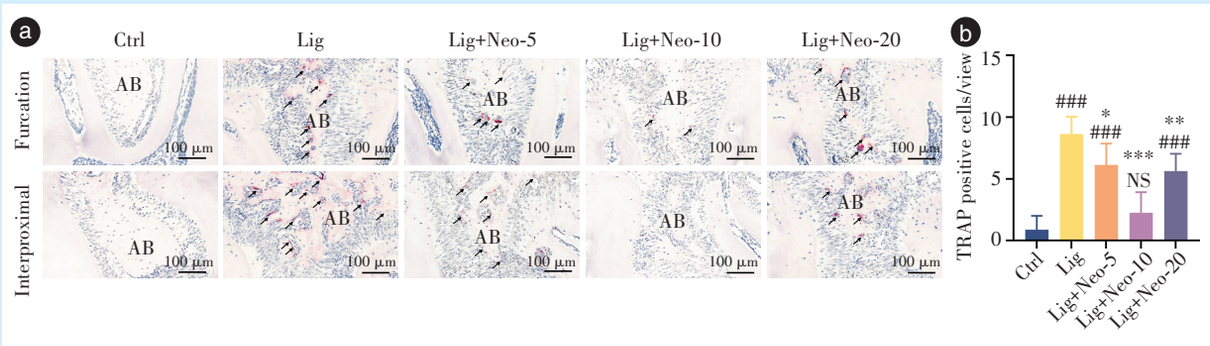

a: TRAP staining images of the furcation area and distal approximal surface of the maxillary second molars in mice from each group. Arrows indicate osteoclasts (TRAP-positive cells). Scale bar = 100 μm. b: quantification of osteoclast numbers in TRAP staining. Ctrl group: mice received saline gavage without silk ligation; Lig group: mice with silk ligation received saline gavage; Lig + Neo-5 group: mice with silk ligation received 5 mg/kg Neo gavage; Lig + Neo-10 group: mice with silk ligation received 10 mg/kg Neo gavage; Lig + Neo-20 group: mice with silk ligation received 20 mg/kg Neo gavage. Neo: neoeriocitrin; AB: alveolar bone; TRAP: tartrate-resistant acid phosphatase. Compared with the Ctrl group, ###: $P < 0.001$, NS: $P > 0.05$. Compared with the Lig group, *: $P < 0.05$, **: $P < 0.01$, ***: $P < 0.001$

Figure 3　Effect of neoeriocitrin on osteoclasts in periodontal tissue from mice with periodontitis

图3　新北美圣草苷对牙周炎小鼠牙周组织中破骨细胞的影响

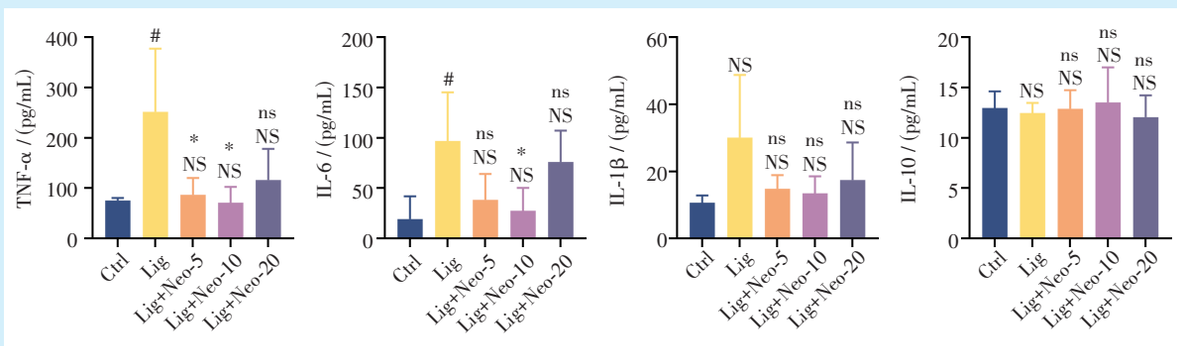

Serum concentrations of TNF-α, IL-6, IL-1β, and IL-10 detected by ELISA in each group. Ctrl group: mice received saline gavage without silk ligation; Lig group: mice with silk ligation received saline gavage; Lig + Neo-5 group: mice with silk ligation received 5 mg/kg Neo gavage; Lig + Neo-10 group: mice with silk ligation received 10 mg/kg Neo gavage; Lig + Neo-20 group: mice with silk ligation received 20 mg/kg Neo gavage. Neo: neoeriocitrin; ELISA: enzyme-linked immunosorbent assay; TNF-α: tumor necrosis factor-α; IL-6: interleukin-6; IL-1β: interleukin-1β; IL-10: interleukin-10. Compared with the Ctrl group, #: $P < 0.05$, NS: $P > 0.05$; Compared with the Lig group, *: $P < 0.05$, ns: $P > 0.05$

Figure 4　Effect of neoeriocitrin on serum inflammatory cytokine levels in mice with periodontitis

图4　新北美圣草苷对牙周炎小鼠血清炎症因子水平的影响

效调节这一变化(图5b)。物种组成分析显示,在门水平上,各组优势菌门均为*Bacteroidota*和*Firmicutes*(图5c)。在科水平上,与对照组相比,牙周炎模型组中*Muribaculaceae*和*Erysipelotrichaceae*的相对丰度降低,*Bacteroidaceae*的丰度升高;Neo干预逆转了这一趋势(图5d)。在属水平上,牙周炎模型组中*Allobaculum*的丰度降低,*Bacteroides*的丰度显著升高,*Lactobacillus*的丰度略微升高;Neo给药后,*Allobaculum*和*Lactobacillus*的丰度显著升高,而*Bacteroides*的丰度则降至对照组水平以下(图5e)。LEfSe分析(LDA > 3)发现,*Bacteroides*是牙周炎模型组的标志性菌属,而*Butyricimonas*则在Lig+Neo-10组中显著富集(图5f&5g)。上述结果表明,Neo通过调节牙周炎小鼠的肠道菌群组成与结构,逆转其失调状态。其保护作用可能与富集益生菌(如*Lactobacillus*、*Allobaculum*)、抑制机会致病菌(如*Bacteroides*)的异常增殖,并促进产丁酸菌(如*Butyricimonas*)的生长密切相关。

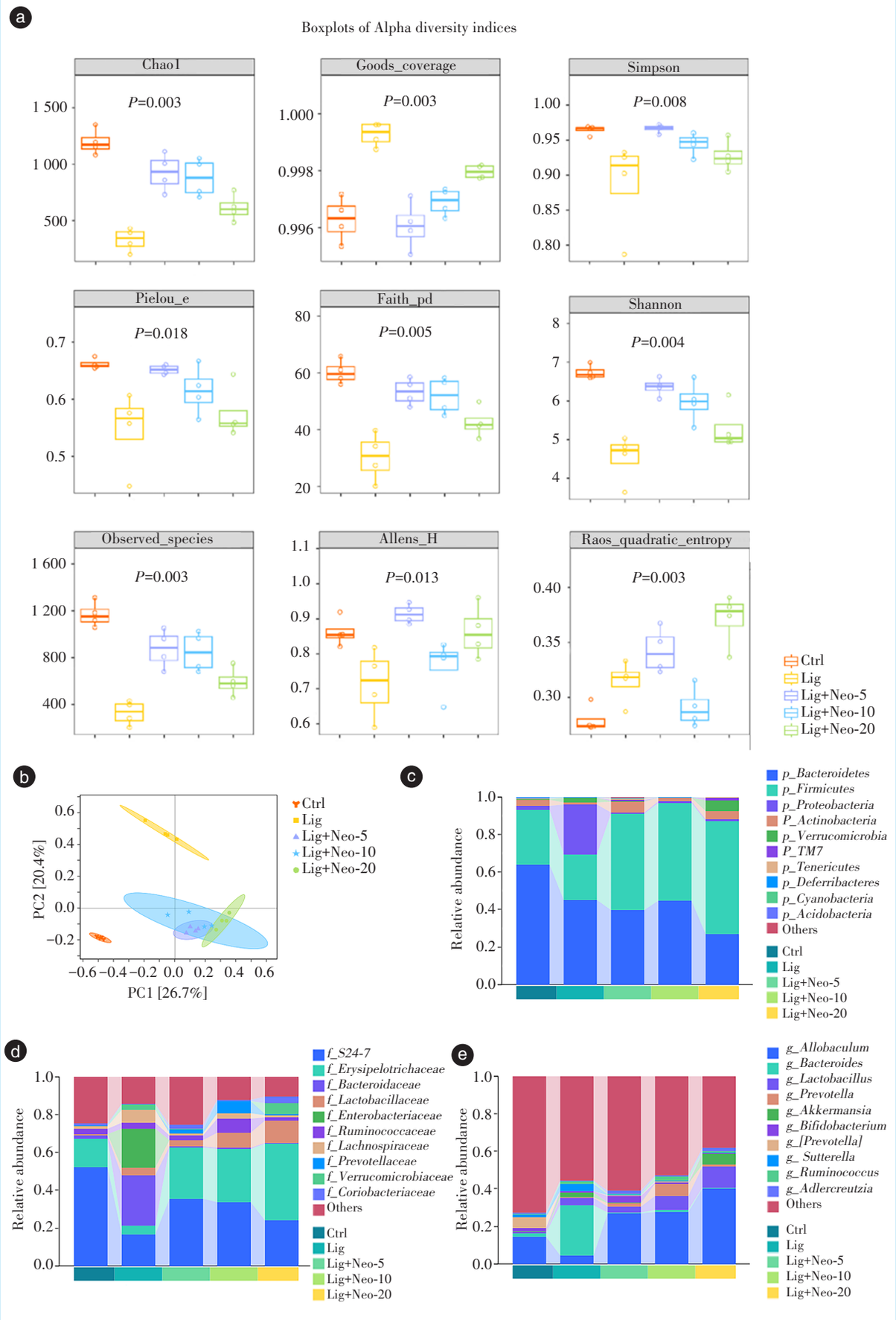
a
Boxplots of Alpha diversity indices
Chao1
P=0.003
Goods_coverage
P=0.003
Simpson
P=0.008
Pielou_e
P=0.018
Faith_pd
P=0.005
Shannon
P=0.004
Observed_species
P=0.003
Allens_H
P=0.013
Raos_quadratic_entropy
P=0.003
Ctrl
Lig
Lig+Neo-5
Lig+Neo-10
Lig+Neo-20
b
PC2 [20.4%]
PC1 [26.7%]
c
Relative abundance
p_Bacteroidetes
p_Firmicutes
p_Proteobacteria
P_Actinobacteria
p_Verrucomicrobia
P_TM7
p_Tenericutes
p_Deferribacteres
p_Cyanobacteria
p_Acidobacteria
Others
d
f_S24-7
f_Erysipelotrichaceae
f_Bacteroidaceae
f_Lactobacillaceae
f_Enterobacteriaceae
f_Ruminococcaceae
f_Lachnospiraceae
f_Prevotellaceae
f_Verrucomicrobiaceae
f_Coriobacteriaceae
Others
e
g_Allobaculum
g_Bacteroides
g_Lactobacillus
g_Prevotella
g_Akkermansia
g_Bifidobacterium
g_[Prevotella]
g_ Sutterella
g_Ruminococcus
g_Adlercreutzia
Others

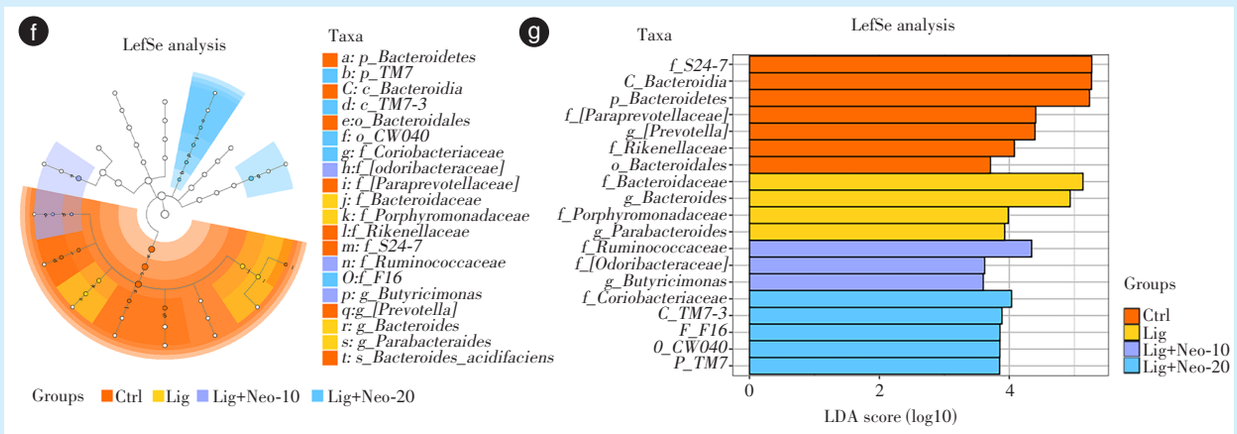

a: comparison of gut microbiota alpha diversity indices (such as Chao1, Shannon) among groups. b: PCoA analysis based on Bray – Curtis distance. c: heatmap of the top 10 relative abundances at the phylum level. d: heatmap of the top 10 relative abundances at the family level. e: heatmap of the top 10 relative abundances at the genus level. f&g: LefSe analysis of differentially abundant taxa between groups. Ctrl group: mice received saline gavage without silk ligation; Lig group: mice with silk ligation received saline gavage; Lig + Neo-5 group: mice with silk ligation received 5 mg/kg Neo gavage; Lig + Neo-10 group: mice with silk ligation received 10 mg/kg Neo gavage; Lig + Neo-20 group: mice with silk ligation received 20 mg/kg Neo gavage. Neo: neoeriocitrin; PCoA: principal coordinates analysis; LefSe: linear discriminant analysis effect size

Figure 5　Effect of neoeriocitrin on gut microbiota in mice with periodontitis

图5　新北美圣草苷对牙周炎小鼠肠道菌群的影响

2.6　Neo对牙周炎小鼠多器官毒性和肠道屏障功能的影响

为评估Neo的生物学安全性，本研究对小鼠心、肝、脾、肺、肾和结肠组织进行HE染色分析。结果显示，各器官组织结构清晰，细胞形态正常，未见明显病理改变、炎症细胞浸润或毛细血管增生，表明Neo在上述剂量下未显示器官毒性。进一步通过HE和ZO-1免疫组化染色评估肠道屏障功能，发现各组结肠上皮结构完整，ZO-1表达无显著组间差异，提示Neo未引起肠道屏障功能损伤或上皮完整性破坏（图6）。

3　讨　论

牙周炎的核心病理特征是菌斑生物膜引发的过度宿主免疫炎症反应，最终导致牙槽骨吸收和附着丧失[24-25]。近年来，大量研究聚焦于植物来源的天然化合物在调节宿主免疫及控制炎症反应方面的潜力，并将其视为牙周炎辅助治疗的新策略。例如，甜橙黄酮能靶向转录因子Bach1并上调HO-1表达，有效缓解牙周组织氧化应激和炎症反应[26]。根皮素可通过抑制低氧诱导因子-1α（hypoxia inducible factor-1α，HIF-1α）介导的糖酵解和磷脂酰肌醇3-激酶（phosphatidylinositol 3-kinase，PI3K）/蛋白激酶B（protein kinase B，Akt）通路，调节巨噬细胞极化，恢复牙周免疫微环境稳态[27]。其他植物提取物如姜黄素[28]、原花青素[29]和槲皮素[30]在实验性牙周炎中也显示出保护效果。这些研究共同表明，植物天然化合物凭借其多靶点作用与良好安全性的特性，在牙周炎的炎症与骨破坏调控中扮演重要角色。在此背景下，本研究聚焦于另一种黄酮类化合物Neo，并证实其治疗能显著减轻了结扎诱导的牙槽骨丧失。

组织学分析进一步显示，Neo有效缓解了附着丧失、炎症细胞浸润和胶原纤维破坏。尤为重要的是，TRAP染色结果表明10 mg/kg Neo最能显著抑制破骨细胞的生成与活化，表明其骨保护作用具有最佳剂量窗口，可能与直接抑制破骨细胞分化和间接改善促破骨形成的炎症微环境密切相关。本研究中观察到的Neo疗效呈现出明显的剂量依赖性，其中10 mg/kg剂量展现出最优的保护效果，而20 mg/kg剂量在部分指标上效果反而减弱。这一现象与许多天然产物所表现的“毒物兴奋效应”规律相符，即低剂量产生有益刺激而高剂量可能无效或产生抑制效应[31-32]。在牙周炎研究领域，其他黄酮类[33]或多酚类化合物[34]，也报道了类似的最适剂量窗口。笔者推测，10 mg/kg剂量可能在体内达到了最佳的药代动力学平衡，有效激活关键的抗炎与成骨/抗破骨信号通路，同时避免了高剂

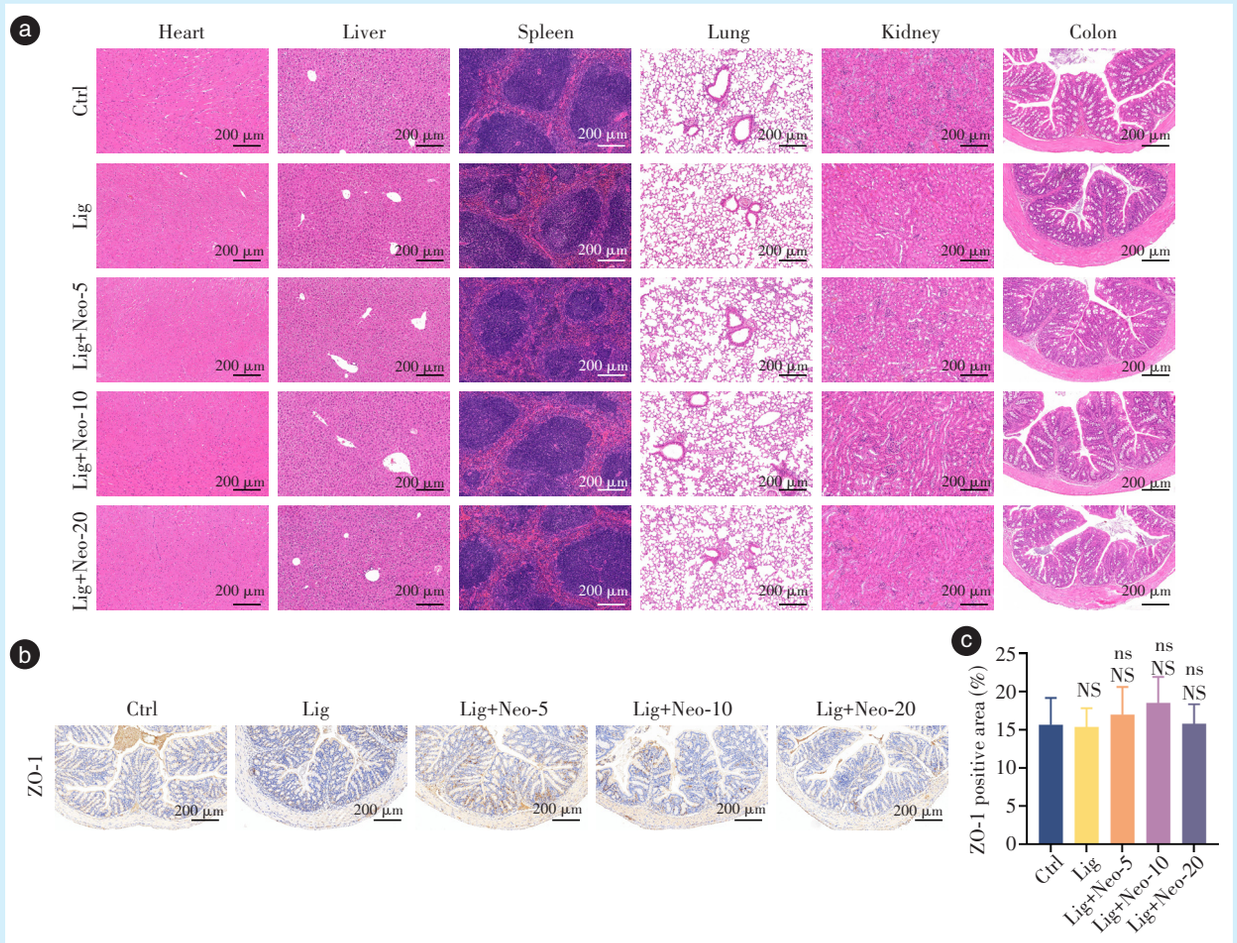

a: HE staining images of heart, liver, spleen, lung, kidney, and colon tissues. Scale bar = 200 μm; b: immunohistochemical staining results of ZO-1 in colon tissue. Scale bar = 200 μm; c: statistical analysis of the percentage area of ZO-1 positive expression. Ctrl group: mice received saline gavage without silk ligation; Lig group: mice with silk ligation received saline gavage; Lig + Neo-5 group: mice with silk ligation received 5 mg/kg Neo gavage; Lig + Neo-10 group: mice with silk ligation received 10 mg/kg Neo gavage; Lig + Neo-20 group: mice with silk ligation received 20 mg/kg Neo gavage. Neo: neoeriocitrin; ZO-1: zonula occludens-1. Compared with the Ctrl group, NS: $P > 0.05$; Compared with the Lig group, ns: $P>0.05$

Figure 6　Effect of neoeriocitrin on multi-organ toxicity and intestinal barrier function in mice with periodontitis

图6　新北美圣草苷对牙周炎小鼠多器官毒性和肠道屏障功能的影响

量下可能出现的非特异性细胞效应或信号饱和。

此外，牙周炎不仅引起局部组织破坏，还会导致肠道菌群失调[35-36]。本研究16S rRNA测序分析发现，牙周炎小鼠肠道菌群的α多样性和β多样性均发生显著改变，而Neo干预能有效逆转这一紊乱。值得注意的是，虽然所有剂量的Neo均能升高益生菌（如*Lactobacillus*，*Allobaculum*）的丰度并抑制机会致病菌（如*Bacteroides*）的增殖，但只有10 mg/kg剂量能特异性地、显著地富集了*Butyricimonas*。这一发现具有重要的机制提示意义，因为该菌是一种能够产生丁酸的关键有益菌。丁酸在体内以丁酸盐的形式存在。丁酸盐是维持肠道屏障功能的核心代谢物[37]，更重要的是，它能进入循环系统，通过多种机制对骨代谢产生积极的调节作用。例如，丁酸盐可作为组蛋白去乙酰化抑制剂调控免疫细胞功能，影响炎性细胞因子的表达水平，抑制破骨细胞生成[38]；同时，丁酸盐也能通过激活G蛋白偶联受体或影响骨保护素（osteoprotegerin，OPG）/RANKL轴来调控骨重塑[39-40]。这与本研究观察到的10 mg/kg Neo组血清TNF-α和IL-6水平被最有效降低、破骨细胞数量显著减少的结果高度吻合。因此本研究推测10 mg/kg Neo可能通过特异性富集产丁酸的*Butyricimonas*，经由“口—肠—骨轴”介导其卓越的骨保护效应，这为不同剂量组间的表型差异提供了合理的机制解释。

本研究也存在一定的局限性。①本研究作为

Neo治疗牙周炎的首次系统性功效验证，未设置阳性对照药物组，其在疗效谱中的相对优势有待后续研究进行横向比较。②血清炎症因子结果虽显示出有统计学意义的下降趋势，但个体差异较大，且本研究未检测丙氨酸氨基转移酶/天门冬氨酸氨基转移酶、尿素氮和肌酐比值等血清生化指标以及系统的体重与状态评分。尽管对心、肝、脾、肺、肾的组织学检查未发现任何明显的毒性病理改变，为排除严重的毒性与应激干扰提供了关键的形态学证据，但未来研究仍建议纳入上述生化与生理指标，以更精确地评估其全身性影响。③尽管本研究观察到Neo对肠道菌群有显著的调节作用，但其具体是通过直接作用于肠道微生物，还是通过减轻口腔炎症间接影响“口-肠轴”，尚需通过粪菌移植等实验进一步验证。④当前采用的全身给药方式旨在探索其系统性效应，未来的研究将重点探索将其制备成局部缓释制剂的可行性，以更好地贴合临床治疗需求。⑤Neo发挥保护作用所涉及的具体分子靶点和下游信号通路网络，尚需在细胞与分子层面进行更深入的解析。最后，口腔菌群在本研究中没有被同步分析，未能直接揭示“口-肠轴”双向互作的详细机制。

综上所述，本研究从局部到全身、从组织到微生物组，系统地揭示了10 mg/kg Neo对实验性牙周炎的多重保护效应。其作用机制不仅局限于局部的抗炎和抑制骨吸收，还可能涉及通过“口-肠轴”调节肠道菌群和系统免疫。结合其优异的安全性，Neo有望成为一种极具开发前景的牙周炎辅助治疗药物。未来的研究将聚焦于阐明其特定剂量下的具体分子机制，并探索其与其他治疗方法联合应用的协同效应。

【Author contributions】 Wu Y performed the experiments, analyzed the data and wrote the article. Yuan ZY, and Zhang YH revised the article. Yan FH designed the study and revised the article. All authors read and approved the final manuscript submitted.

参考文献

[1] Papapanou PN, Sanz M, Buduneli N, et al. Periodontitis: consensus report of workgroup 2 of the 2017 world workshop on the classification of periodontal and peri-implant diseases and conditions [J]. J Periodontol, 2018, 89(Suppl 1): S173-S182. doi: 10.1002/JPER.17-0721.

[2] Kinane DF, Stathopoulou PG, Papapanou PN. Periodontal diseases [J]. Nat Rev Dis Primers, 2017, 3: 17038. doi: 10.1038/nrdp.2017.38.

[3] Li A, Chen L, Thomas RZ, et al. Periodontal breakdown intertooth relationships in estimating periodontitis-related tooth loss[J]. J Dent, 2021, 112: 103755. doi: 10.1016/j.jdent.2021.103755.

[4] Wang RP, Huang J, Chan KWY, et al. IL-1β and TNF-α play an important role in modulating the risk of periodontitis and Alzheimer's disease[J]. J Neuroinflammation, 2023, 20(1): 71. doi: 10.1186/s12974-023-02747-4.

[5] Wang N, Zheng L, Qian J, et al. Salivary microbiota of periodontitis aggravates bone loss in ovariectomized rats[J]. Front Cell Infect Microbiol, 2022, 12: 983608. doi: 10.3389/fcimb.2022.983608.

[6] Qian J, Lu J, Huang Y, et al. Periodontitis salivary microbiota worsens colitis[J]. J Dent Res, 2022, 101(5): 559-568. doi: 10.1177/00220345211049781.

[7] Rams TE, Sautter JD, van Winkelhoff AJ. Emergence of antibiotic-resistant *Porphyromonas gingivalis* in United States periodontitis patients[J]. Antibiotics (Basel), 2023, 12(11): 1584. doi: 10.3390/antibiotics12111584.

[8] Gager Y, Koppe J, Vogl I, et al. Antibiotic resistance genes in the subgingival microbiome and implications for periodontitis therapy [J]. J Periodontol, 2023, 94(11): 1295-1301. doi: 10.1002/JPER.22-0696.

[9] Lu H, He L, Jin D, et al. Effect of adjunctive systemic antibiotics on microbial populations compared with scaling and root planing alone for the treatment of periodontitis: a pilot randomized clinical trial[J]. J Periodontol, 2022, 93(4): 570-583. doi: 10.1002/JPER.20-0764.

[10] Xu X, Lu H, Huo P, et al. Effects of amoxicillin and metronidazole as an adjunct to scaling and root planing on glycemic control in patients with periodontitis and type 2 diabetes: a short-term randomized controlled trial[J]. J Periodontal Res, 2024, 59(2): 249-258. doi: 10.1111/jre.13225.

[11] Cai G, Ren L, Yu J, et al. A microenvironment-responsive, controlled release hydrogel delivering embelin to promote bone repair of periodontitis *via* anti-infection and osteo-immune modulation[J]. Adv Sci (Weinh), 2024, 11(34): e2403786. doi: 10.1002/advs.202403786.

[12] Li N, Wang B, Yang M, et al. The multi-target action mechanism for the anti-periodontitis effect of astragali radix based on bioinformatics analysis and *in vitro* verification[J]. Nutrients, 2025, 17(4): 627. doi: 10.3390/nu17040627.

[13] Chen H, Liu Y, Yu S, et al. Cannabidiol attenuates periodontal inflammation through inhibiting TLR4/NF-κB pathway[J]. J Periodontal Res, 2023, 58(4): 697-707. doi: 10.1111/jre.13118.

[14] 廖丹, 葛颂. 淫羊藿苷与补肾固齿丸对大鼠慢性牙周炎牙槽骨重建的比较研究[J]. 口腔疾病防治, 2020, 28(12): 759-767. doi: 10.12016/j.issn.2096-1456.2020.12.002.
Liao D, Ge S. Comparative study on icariin and Bu-Shen-Gu-Chi-Wan for alveolar reconstruction in chronic periodontitis in rats[J]. J Prev Treat Stomatol Dis, 2020, 28(12): 759-767. doi: 10.12016/j.issn.2096-1456.2020.12.002.

[15] Ahn JS, Lee CH, Liu XQ, et al. Neuroprotective effects of phenolic constituents from drynariae rhizoma[J]. Pharmaceuticals (Basel), 2024, 17(8): 1061. doi: 10.3390/ph17081061.

[16] Posadino AM, Maccioccu P, Eid AH, et al. Citrus limon var. pom-

pia camarda var. nova: a comprehensive review of its botanical characteristics, traditional uses, phytochemical profile, and potential health benefits[J]. Nutrients, 2024, 16(16): 2619. doi: 10.3390/nu16162619.

[17] Zeng X, Zheng Y, He Y, et al. Microbial metabolism of naringin and the impact on antioxidant capacity[J]. Nutrients, 2022, 14(18): 3765. doi: 10.3390/nu14183765.

[18] Bartella L, Mazzotti F, Talarico IR, et al. Structural characterization of peripolin and study of antioxidant activity of HMG flavonoids from bergamot fruit[J]. Antioxidants (Basel), 2022, 11(10): 1847. doi: 10.3390/antiox11101847.

[19] Li L, Zeng Z, Cai G. Comparison of neoeriocitrin and naringin on proliferation and osteogenic differentiation in MC3T3-E1[J]. Phytomedicine, 2011, 18(11): 985-989. doi: 10.1016/j.phymed.2011.03.002.

[20] Jin H, Jiang N, Xu W, et al. Effect of flavonoids from rhizoma drynariae on osteoporosis rats and osteocytes[J]. Biomed Pharmacother, 2022, 153: 113379. doi: 10.1016/j.biopha.2022.113379.

[21] Wu Y, Liu H, Wang Q, et al. Neoeriocitrin targeting Beclin1 deubiquitination and autophagy in osteogenic differentiation of human dental pulp stem cells[J]. Adv Sci (Weinh), 2025, 12(43): e04378. doi: 10.1002/advs.202504378.

[22] Du N, Song L, Li Y, et al. Phytoestrogens protect joints in collagen induced arthritis by increasing IgG glycosylation and reducing osteoclast activation[J]. Int Immunopharmacol, 2020, 83: 106387. doi: 10.1016/j.intimp.2020.106387.

[23] Chai S, Yang Y, Wei L, et al. Luteolin rescues postmenopausal osteoporosis elicited by OVX through alleviating osteoblast pyroptosis *via* activating PI3K-AKT signaling[J]. Phytomedicine, 2024, 128: 155516. doi: 10.1016/j.phymed.2024.155516.

[24] Xu J, Yu L, Ye S, et al. Oral microbiota-host interaction: the chief culprit of alveolar bone resorption[J]. Front Immunol, 2024, 15: 1254516. doi: 10.3389/fimmu.2024.1254516.

[25] Usui M, Onizuka S, Sato T, et al. Mechanism of alveolar bone destruction in periodontitis - periodontal bacteria and inflammation [J]. Jpn Dent Sci Rev, 2021, 57: 201-208. doi: 10.1016/j.jdsr.2021.09.005.

[26] Yuan Z, Li J, Xiao F, et al. Sinensetin protects against periodontitis through binding to Bach1 enhancing its ubiquitination degradation and improving oxidative stress[J]. Int J Oral Sci, 2024, 16(1): 38. doi: 10.1038/s41368-024-00305-z.

[27] Zeng X, Li T, Yang K, et al. Natural compound phloretin restores periodontal immune homeostasis *via* HIF-1α-regulated PI3K/Akt and glycolysis in macrophages[J]. Int Immunopharmacol, 2024, 141: 112933. doi: 10.1016/j.intimp.2024.112933.

[28] Wang Y, Lin H, Huang W, et al. Curcumin attenuates periodontal injury *via* inhibiting ferroptosis of ligature-induced periodontitis in mice[J]. Int J Mol Sci, 2023, 24(12): 9835. doi: 10.3390/ijms24129835.

[29] Nawrot-Hadzik I, Matkowski A, Kubasiewicz-Ross P, et al. Proanthocyanidins and flavan-3-ols in the prevention and treatment of periodontitis-immunomodulatory effects, animal and clinical studies[J]. Nutrients, 2021, 13(1): 239. doi: 10.3390/nu13010239.

[30] An Y, Zhao R, Liu W, et al. Quercetin through miR-147-5p/Clip3 axis reducing Th17 cell differentiation to alleviate periodontitis[J]. Regen Ther, 2024, 27: 496-505. doi: 10.1016/j.reth.2024.04.016.

[31] Li X, Zhao W, Chen J, et al. Dosage impact of submerged plants extracts on microcystis aeruginosa growth: from hormesis to inhibition[J]. Ecotoxicol Environ Saf, 2023, 268: 115703. doi: 10.1016/j.ecoenv.2023.115703.

[32] Fonseca SSS, S Port's NM, Aguiar GPS, et al. Brosimine B and the biphasic dose-response: insights into hormesis and retinal neuroprotection[J]. Front Pharmacol, 2025, 16: 1558726. doi: 10.3389/fphar.2025.1558726.

[33] Fan Z, Tang P, Bu Y, et al. Luteolin as a multi-target agent against periodontitis: integrating Nrf2-mediated antioxidant defense and quorum sensing interference[J]. Free Radic Biol Med, 2025, 242: 54-67. doi: 10.1016/j.freeradbiomed.2025.10.261.

[34] Li Y, Huang Z, Pan S, et al. Resveratrol alleviates diabetic periodontitis-induced alveolar osteocyte ferroptosis possibly *via* regulation of SLC7A11/GPX4[J]. Nutrients, 2023, 15(9): 2115. doi: 10.3390/nu15092115.

[35] Bao J, Li L, Zhang Y, et al. Periodontitis may induce gut microbiota dysbiosis *via* salivary microbiota[J]. Int J Oral Sci, 2022, 14(1): 32. doi: 10.1038/s41368-022-00183-3.

[36] Lu J, Zhang S, Huang Y, et al. Periodontitis-related salivary microbiota aggravates Alzheimer's disease *via* gut-brain axis crosstalk [J]. Gut Microbes, 2022, 14(1): 2126272. doi: 10.1080/19490976.2022.2126272.

[37] Chen H, Qian Y, Jiang C, et al. Butyrate ameliorated ferroptosis in ulcerative colitis through modulating Nrf2/GPX4 signal pathway and improving intestinal barrier[J]. Biochim Biophys Acta Mol Basis Dis, 2024, 1870(2): 166984. doi: 10.1016/j.bbadis.2023.166984.

[38] He J, Chu Y, Li J, et al. Intestinal butyrate-metabolizing species contribute to autoantibody production and bone erosion in rheumatoid arthritis[J]. Sci Adv, 2022, 8(6): eabm1511. doi: 10.1126/sciadv.abm1511.

[39] Wu L, Luo Z, Chen Y, et al. Butyrate inhibits dendritic cell activation and alleviates periodontitis[J]. J Dent Res, 2023, 102(12): 1326-1336. doi: 10.1177/00220345231187824.

[40] Wu Z, Ding Q, Yue M, et al. Caspase-3/GSDME-mediated pyroptosis leads to osteogenic dysfunction of osteoblast-like cells[J]. Oral Dis, 2024, 30(3): 1392-1402. doi: 10.1111/odi.14579.

（编辑　周春华）

官网